analytical chemistry

pubs.acs.org/ac Article

Real-Time Monitoring of Metal Ions during the Molten Salt Electrolysis Process by Optical Emission Spectrometry Based on Microplasma

Junhan Luo, Jingcui Liu, Qi Qing, Shuang Liu, Zhe Wang,* Jing Chen, and Yuexiang Lu*

Cite This: *Anal. Chem.* 2024, 96, 20406−20413 Read Online

ACCESS | Metrics & More | Article Recommendations

ABSTRACT: Molten salt electrolysis has been widely used in the production and separation of metals, but it still lacks in situ real-time analysis methods to monitor the electrolysis process. In this work, a microplasma spectroscopic real-time analysis (MIPECA) system is developed based on noncontact direct current (DC) glow discharge. With the MIPECA system, the atomic emission spectroscopy of Li and K could be obtained in situ in LiCl−KCl molten salt, and the impact of different operating conditions on spectral signals was investigated. Then, the characteristic spectra of ten representative elements, including alkali metals (Na, Cs), alkaline earth metals (Mg, Ca, Sr, Ba), transition metals (Ag, Cu, Ni), and lanthanide metals (Ce), were all successfully excited for qualitative analysis. Under the optimal operating conditions, quantitative analysis of Ag, Cs, and Sr was achieved with high sensitivity and low limits of detection (LOD) of about 0.063, 0.021, and 0.073 wt %, respectively. Finally, the electrolysis process of Ag^+ in LiCl−KCl molten salt was real-time monitored by using this MIPECA system, showing its application potential in molten salt electrolysis.

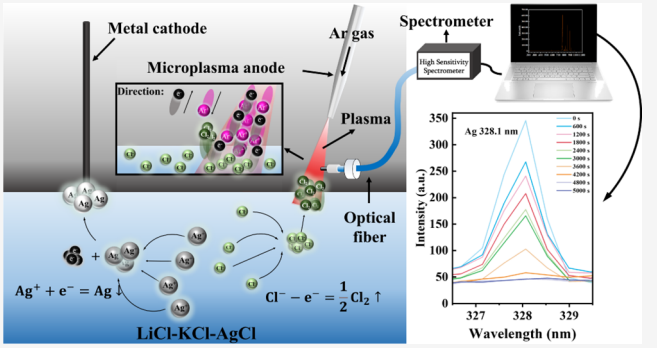

INTRODUCTION

Molten salt, defined as a fused substance resulting from the melting of salts at elevated temperatures, primarily comprises metal cations and nonmetal anions, constituting an excellent electrolytic medium. In comparison to aqueous solutions, molten salts exhibit a broader electrochemical window,[1] rendering them suitable for the extraction and refining of active metals, such as aluminum, sodium, magnesium, lithium, and other alkali and alkaline earth metals.[2,3] The extraction of active metals from molten salt electrolysis has become the predominant production method. Additionally, due to its higher electrical conductivity, relative stability at high temperatures, and resistance to radiation, molten salt finds applications in spent nuclear fuel reprocessing, in which electrolysis is used for the separation of radioactive metal ions and the refining of uranium.[4−7] During these electrolysis processes, it is necessary to analyze the ion species and concentration in molten salt in order to monitor the reactions and guarantee operation safety. Nevertheless, challenges associated with the high-temperature operation of molten salts, the potential generation of corrosive gases during electrolysis, and issues like component volatility make in situ accurate measurement of molten salt components difficult.[8]

In conventional processes, sampling and subsequent offline analysis of sample composition using techniques such as inductively coupled plasma atomic emission spectrometry (ICP-AES) are commonly employed after timed molten salt sampling.[9,10] However, this method suffers from significant drawbacks. First, protracted chemical separation steps inevitably introduce errors into the system, thereby affecting the accuracy of test results. Second, even with reliable test results, the substantial time required for the processing steps leads to data lag, preventing practical guidance for the electrolysis process. Lastly, the need to interrupt reactions during sample collection affects the reaction continuity and may even induce unknown side reactions.

It has been reported that electrochemical methods[11,12] may be suitable for in situ operation in molten salt. However, interference in multicomponent mixtures poses challenges for stable analysis. Spectroscopic analysis methods such as laser-induced breakdown spectroscopy (LIBS),[13−15] ultraviolet−visible spectroscopy (UV−vis),[16,17] and Raman spectroscopy (RS)[18] may also hold promise for in situ analysis of molten

Received: July 30, 2024
Revised: November 29, 2024
Accepted: December 5, 2024
Published: December 17, 2024

https://doi.org/10.1021/acs.analchem.4c04004
Anal. Chem. 2024, 96, 20406−20413

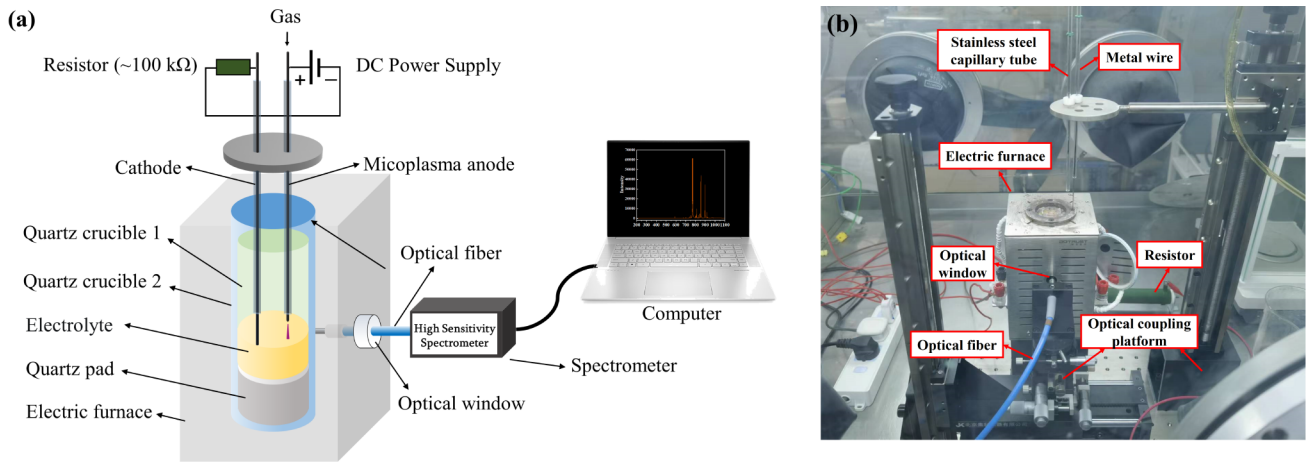

Figure 1. Specific device for the MIPECA system in molten salt. (a) Schematic view and (b) photograph.

salts. Nevertheless, LIBS equipment is overall bulky, expensive, and faces difficulties in addressing sample splashing caused by shockwaves.[14] UV−vis methods also struggle with stability in complex systems and inaccuracies in measuring high-concentration elements. To the best of our knowledge, a reliable method for real-time monitoring of molten salt composition has yet to be attempted.

Direct current atmospheric pressure glow discharge (DC-APGD) has been extensively explored as an excitation source in optical emission spectroscopy (OES) since 1993 by Cserfalvi and Mezei. But up to now, the study of OES based on DC-APGD predominantly focuses on aqueous systems.[19−26] There are only a few reports on the OES studies in high-temperature molten salt systems.[27,28] In our previous work, we have found that microplasma based on direct current glow discharge can be used as a kind of gaseous electrode for molten salt electrolysis and it has been used for the electrodeposition of metal, metal alloy, and metal oxide.[10,29] At the same time, the microplasma could act as an excitation source of atomic emission spectroscopy of metal ions in molten salt, showing its potential for the simultaneous monitoring of changes in the types and concentrations of elements in electrolyte matrices while facilitating electrochemical reactions.[27,28] However, the study of microplasma in molten salt analysis is still very rare. To realize in situ real-time monitoring of the electrolysis process, it is highly needed to build related equipment, obtain fundamental data, optimize the operation conditions, and establish data analysis methods.

Herein, we present a microplasma spectroscopic real-time analysis (MIPECA) system based on noncontact DC glow discharge in molten salt. The plasma signals excited during the electrolysis process serve as the adsorption of the OES radiation source, achieving mutual coupling between the plasma excitation unit and the optical radiation acquisition unit (Figure 1). The capabilities and differences of microplasma cathodes and anodes to excite OES signals were systematically investigated under different environmental atmospheres. Subsequently, the overall system parameters were optimized. Then, the characteristic spectra of ten representative elements were obtained for qualitative analysis, and three of them were used for assessing the quantitative analysis performance. Finally, the electrolytic reduction process of Ag^+ was monitored in real-time by using a MIPECA system.

EXPERIMENTAL SECTION

Instrumentation. The specific device of the MIPECA system is shown in Figure 1. It consists of a plasma excitation unit and an optical radiation acquisition unit. In the plasma excitation unit, a hollow stainless steel tube (diameter ~1.60 mm) was used as an electrode to induce microplasma, and an inert metal (Mo or Pt) wire (99.99% purity, diameter 1.0 mm) was used as another electrode. All electrodes were thoroughly polished using silicon carbide paper, placed in ethanol, and cleaned by ultrasound. During the experimental process, the plasma was ignited by flowing argon gas (99.0% purity) through controlling the distance between the microplasma electrode and the surface of molten salt at a suitable distance and applying a DC voltage. To fix and protect the hollow tube and improve the stability of plasma excitation, quartz tubes (outer diameter of 4.0 mm and inside diameter of 2.0 mm) were placed outside the hollow tube and metal wire. Moreover, a relatively large resistor (~100 kΩ) was provided to ensure a steady discharge.

In the optical radiation acquisition unit, an optical fiber probe (QP600-2-SR, Ocean Optics Inc., USA) was inserted into the furnace through a custom optical window and was in contact with quartz crucible 2 as much as possible. The surface height of the molten salt was adjusted by a quartz pad (outer diameter of 17.0 mm) to ensure that the plasma signal could be observed in the optical window. At the same time, the positions of the furnace, the optical fiber, and the electrode were precisely fine-tuned by a customized optical coupling platform to further improve the stability of signal reception. Such a scheme can greatly enhance the strength of the signal and ensure flexibility of the signal collection. The optical fiber probe was coupled to the spectrometer (Maya 2000 Pro, Ocean Optics Inc., USA), the data was analyzed by a computer, and the integration time was set to 10 ms. The argon atmosphere experiments were carried out in an argon atmosphere (less than 2.0 ppm of O_2 and H_2O) glovebox.

Reagents and Sample Preparation. All chemicals were of analytical grade or higher. Anhydrous NaCl (99.8% purity) and $CeCl_3$ (99.9% purity) were purchased respectively from Zancheng (Tianjin) Technology Co., Ltd. and Meryer (Shanghai) Chemical Technology Co., Ltd. Anhydrous $MgCl_2$ (99.9% purity) and $CaCl_2$ (99.9% purity) were purchased from Shanghai Macklin Biochemical Technology Co., Ltd. Anhydrous $NiCl_2$ (98.0% purity), $CuCl_2$(98.0%

https://doi.org/10.1021/acs.analchem.4c04004
Anal. Chem. 2024, 96, 20406−20413

purity), AgCl (98.0% purity), CsCl (99.9% purity), $SrCl_2$ (99.9% purity), and $BaCl_2$ (99.99% purity) were purchased from Anhui Senrise Technology Co., Ltd. LiCl (analytical-grade, Anhui Senrise Technology Co., Ltd.) and KCl (analytical-grade, Sinopharm Chemical Reagent Co., Ltd.) easily absorb water in the air. To ensure the stability of the spectral collection, the salt needs to be pretreated first. A mixture of LiCl−KCl eutectic salt (58.8:41.2 mol %) was placed in quartz crucible 1 (outer diameter 17.0 mm, height 65.0 mm) and then dried at 200 °C under vacuum for more than 24 h to remove adsorbed water in the salt. Crucible 1 was then put inside quartz crucible 2 (outer diameter of 22.0 mm, height of 110.0 mm) and placed together in a custom optical electric furnace.

RESULTS AND DISCUSSION

Impact of Operating Parameters on the Emission Spectrum of LiCl−KCl Molten Salt. LiCl−KCl molten salt, with the advantages of a low melting point (355 °C), high conductivity, and cost-effectiveness, has been widely applied in electrorefining, especially for the pyroprocessing of spent nuclear fuel. Therefore, LiCl−KCl molten salt was chosen as the reaction medium to collect the spectroscopic signals. As microplasma can act as both an anode and a cathode and the electrolysis might be operated under air or argon atmospheres, the spectra under four conditions were collected. In the experiment, the molten salt for each batch was individually reconfigured, and both the microplasma and metal electrodes were thoroughly cleaned after completing each set of experiments. The corresponding experimental data are shown in Figure 2. The results indicate that characteristic emission

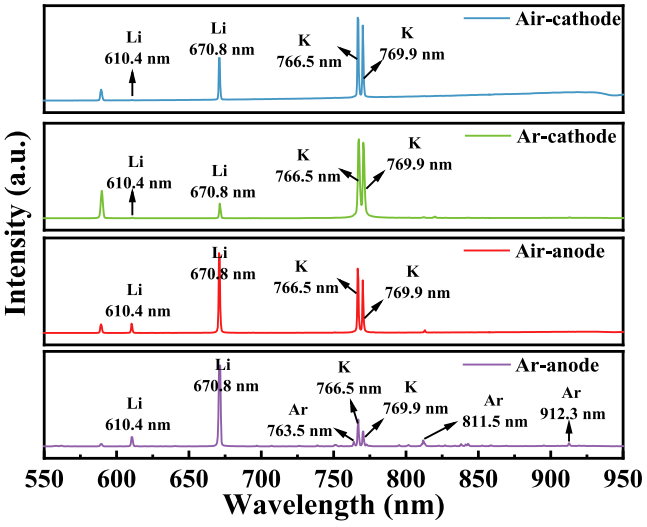

Figure 2. Emission spectrum of LiCl−KCl molten salt generated by microplasma under different conditions.

lines of Li and K can be clearly detected under all four conditions with intensities significantly higher than the background emission, while there are still differences in the emission spectra. To ensure the intensity of the element's characteristic peaks is as strong as possible, it is necessary to select an optimal operating condition and explore the potential factors that may affect the spectral signal.

Compared to the emission spectra excited by the anode, the spectrum excited by the microplasma cathode showed a small change in the intensity of the characteristic peak of K, while the intensity of the characteristic peak of Li decreased significantly. In the anode spectrum, Li 670.8 nm was the highest peak in the entire spectrum, whereas in the cathode spectrum, it was K 766.5 nm. The emission spectra excited by the microplasma electrode also exhibited certain differences under different atmospheric conditions. The characteristic peaks of argon, concentrated in the range of approximately 700−950 nm, could be collected when the microplasma anode was used in an argon atmosphere. In contrast, the microplasma cathode excited in an argon atmosphere did not show obvious argon characteristic peaks. Its emission spectrum was still dominated by the characteristic peaks of Li and K, but compared to the air conditions, the intensity of the Li characteristic peak further decreased. After comprehensive and comparative consideration, we finally chose the emission spectra excited by the microplasma anode in an air atmosphere as the research target.

Then, by choosing the Li 610.4 nm characteristic peak as the reference, the influence of the molten salt temperature, discharge current, and discharge distance on the MIPECA system was studied.

It was found that the spectral intensity was not sensitive to either the discharge distance or the molten salt temperature (Figure 3a,b). However, with the increase in discharge current, the spectral intensity significantly increased, showing a good linear relationship (Figure 3c), consistent with the experimental results of Wei et al. and Greda et al.[19,24] Taking into account all these outcomes, a discharge current of 10 mA, a molten salt temperature of 550 °C, and a discharge distance of 2.0 mm were recognized as optimal and used in the further part of the work.

The response relationship between the plasma excitation unit and the optical radiation acquisition unit was also studied by controlling the discharge switch. The characteristic peak of Li responded in real-time with the plasma turning on and off, as shown in Figure 3d. When the plasma was ignited, the signal stabilized immediately, and after several cycles, the system still exhibited good repeatability, with no significant change in the intensity of the characteristic peak with the relative standard deviation (RSD) less than 3.0%. This rapid and stable spectral responsiveness proved the stability of the MIPECA system, which is a prerequisite for element quantification analysis and real-time monitoring.

Elemental Qualitative Analysis. To verify the feasibility of qualitative analysis of different metal elements in molten salt by microplasma electrodes, alkali metals (Na, Cs), alkaline earth metals (Mg, Ca, Sr, Ba), transition metals (Ag, Cu, Ni), and lanthanide metals (Ce) were added individually into the LiCl−KCl molten salt by using their metal chlorides. The emission spectra excited by the microplasma anode were collected under an air atmosphere in the range of 200−1100 nm. The distribution of element characteristic peaks is related to the arrangement of electron energy levels,[30] so different target elements were analyzed according to the group in the periodic table of elements.

Na and Cs were selected as representatives of alkali metals. Figure 4a showed the spectral data of NaCl in LiCl−KCl. Compared with the emission spectra of the LiCl−KCl blank molten salt, the characteristic peaks of Na at 819.5 nm appeared. Moreover, the intensity of another Na characteristic peak at 589.6 nm was significantly higher. Figure 4b showed the obvious Cs characteristic peaks at 852.1 and 894.3 nm, and the intensity of 852.1 nm was higher.

https://doi.org/10.1021/acs.analchem.4c04004
Anal. Chem. 2024, 96, 20406−20413

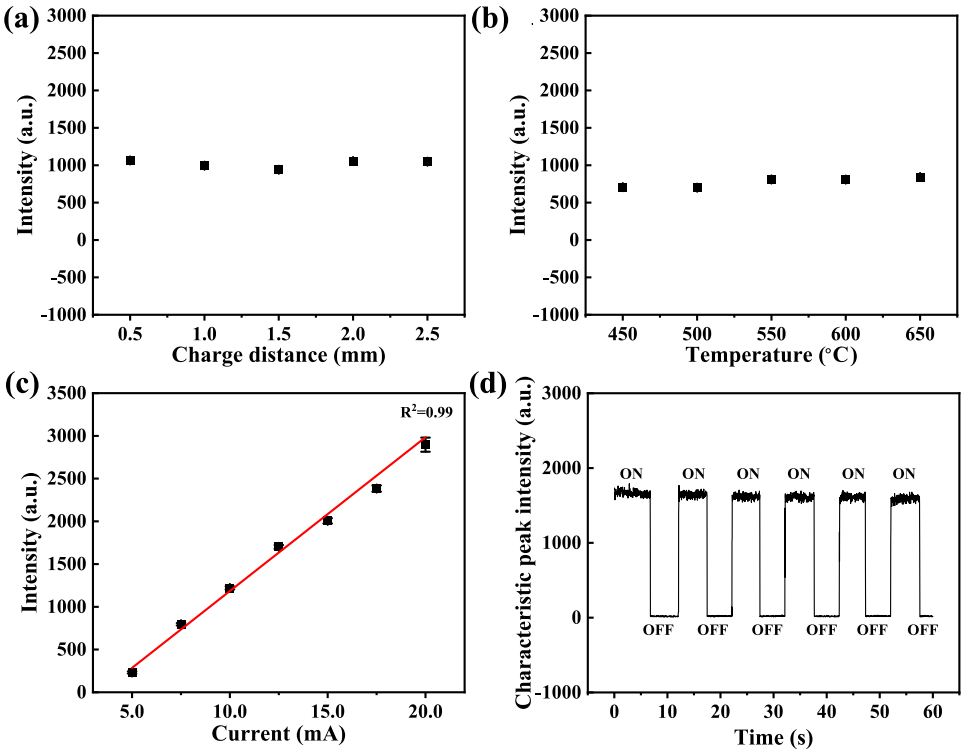

Figure 3. Effects of (a) discharge distance (discharge current 10 mA, molten salt temperature 550 °C), (b) molten salt temperature (discharge distance 2.0 mm, discharge current 10 mA), and (c) discharge current (discharge distance 2.0 mm, molten salt temperature 550 °C) on the signal intensity of Li 610.4 nm. The response relationship between the plasma excitation unit and the optical radiation acquisition unit (d).

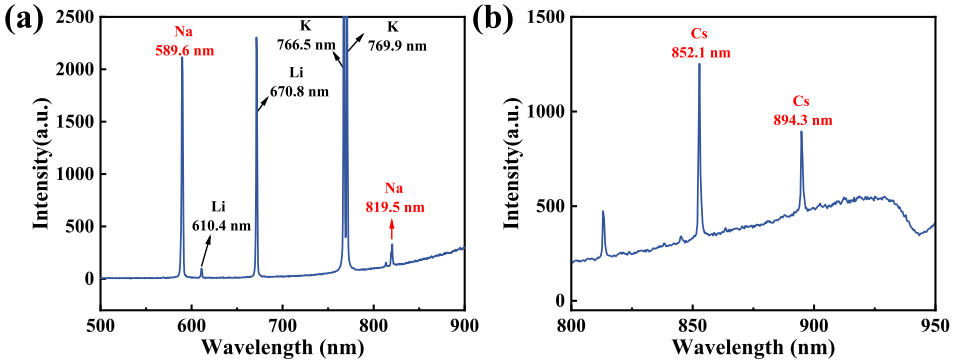

Figure 4. Emission spectra of (a) Na and (b) Cs excited by the microplasma anode in the air.

Mg, Ca, Sr, and Ba were selected as the representatives of the alkaline earth metals. Through collection of the emission spectra, the characteristic peaks of these elements were successfully acquired. As shown in Figure 5, for Mg, only three characteristic peaks at 285.2, 383.8, and 518.4 nm were observed. While, for Ca, Sr, and Ba, much more characteristic peaks were detected in the wavelength range of 400−800 nm. The two main peaks with higher intensity were 616.2 and 422.7 nm for Ca, 661.7 and 460.7 nm for Sr, and 553.5 and 455.4 nm for Ba. In general, compared with alkali metals, alkaline earth metals have more characteristic peaks and lower intensities.

Ag, Cu, and Ni were selected as the representatives of transition metals, while Ce was chosen as the representative of the lanthanide metals. Figure 6a showed the characteristic peaks of Ag at 328.1 338.3, 520.9, and 546.5 nm with strong intensities. Figure 6b showed the characteristic peaks of Cu at 324.8 327.4, 510.6, 515.3, and 521.9 nm. Figure 6c showed a series of characteristic peaks of Ni in the range of 200−400 nm. Figure 6d showed the characteristic peaks of Ce at 425.6 429.0, 522.3, and 524.6 nm.

All the above results indicate that the microplasma electrodes can achieve qualitative analysis of various metal elements in molten salt.

Elemental Quantitative Analysis. To study the quantitative analysis performance of the MIPECA system, Cs, Sr, and Ag were selected as the representatives of alkali metal, alkaline earth metal, and transition metal. The peaks of Cs 852.1 nm, Sr 661.7 nm, and Ag 546.6 nm with high intensity and less noise peak interference were chosen for analysis. While the peak intensity of Li 610.4 nm was moderate, there was no concern about being out of range; therefore, Li 610.4 nm was chosen as the internal reference for Cs and Ag. As for Sr, according to the experimental results, the intensity of K 766.5 nm was more stable in this situation and more suitable to be an internal reference than Li 610.4 nm.

https://doi.org/10.1021/acs.analchem.4c04004
Anal. Chem. 2024, 96, 20406−20413

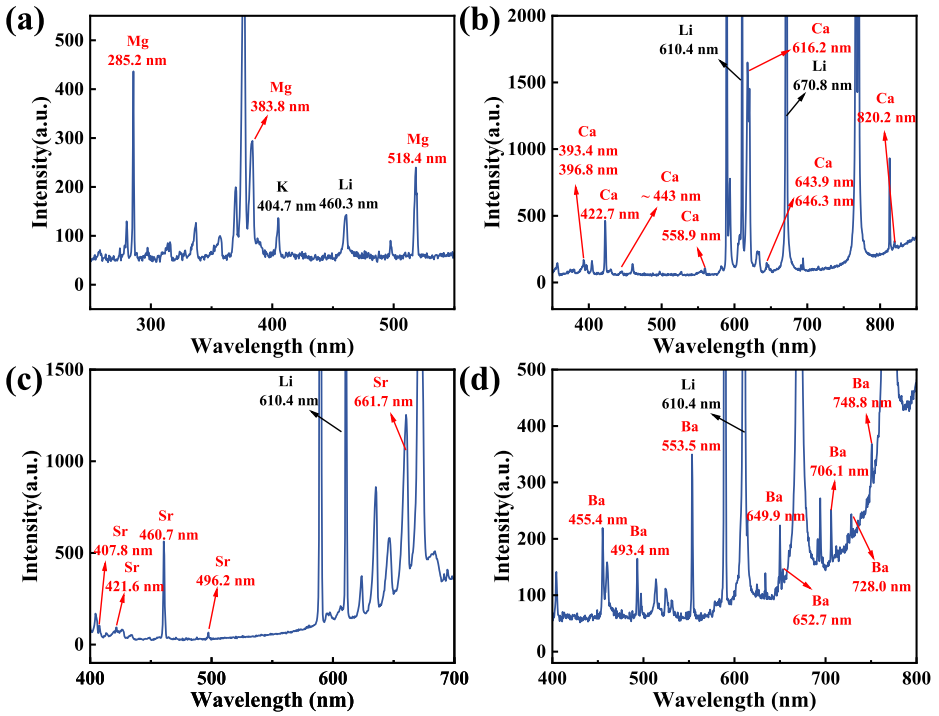

Figure 5. Emission spectra of (a) Mg, (b) Ca, (c) Sr, and (d) Ba excited by the microplasma anode in the air.

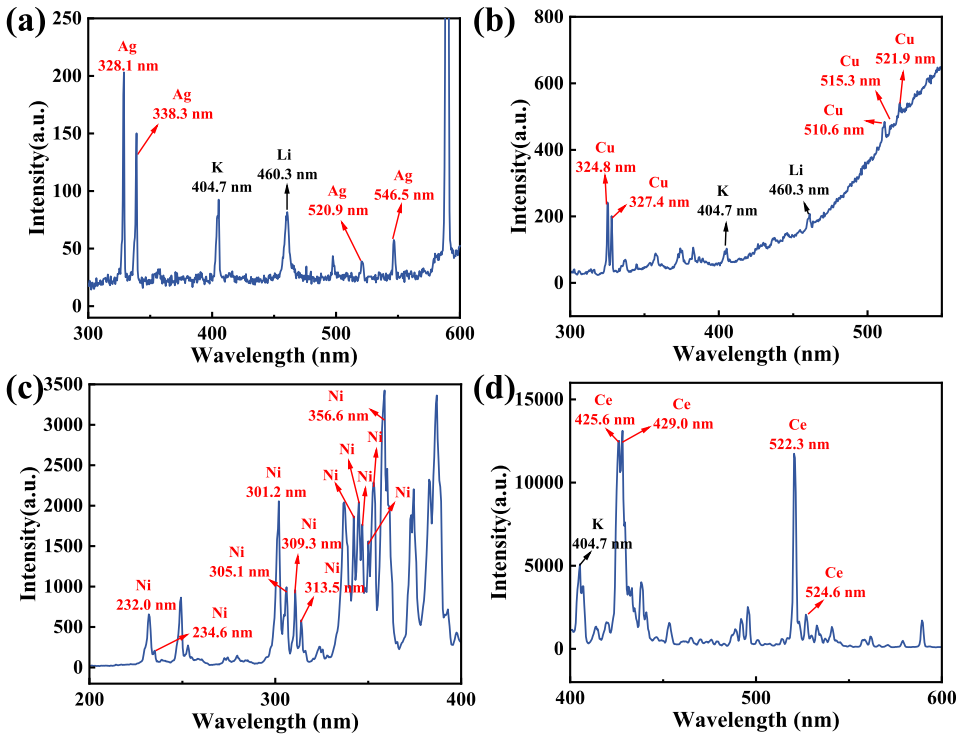

Figure 6. Emission spectra of (a) Ag, (b) Cu, (c) Ni, and (d) Ce excited by the microplasma anode in the air.

The concentration−intensity response relationships of these three elements in LiCl−KCl molten salt were determined at different concentrations from 0.1 to 20 wt %. For different metal elements, the quantitative results exhibited a similar tendency (Figure 7). The relative emission intensities of elements increased with increasing concentration and were linear in different concentration ranges. Within a smaller concentration range, the trend of the spectral intensity increasing with concentration was more pronounced. As the concentration gradually increased, the increasing trend gradually decreased, showing a linear relationship with a lower slope. This phenomenon was consistent with the findings of Wei et al.[28] and was believed to be due to the self-absorption of elements at high concentrations.

Figure 7b,c was the calibration curves established in Cs concentration ranges of 5.0 wt % to 20.0 and 0.1 wt % to 2.0 wt

https://doi.org/10.1021/acs.analchem.4c04004
Anal. Chem. 2024, 96, 20406−20413

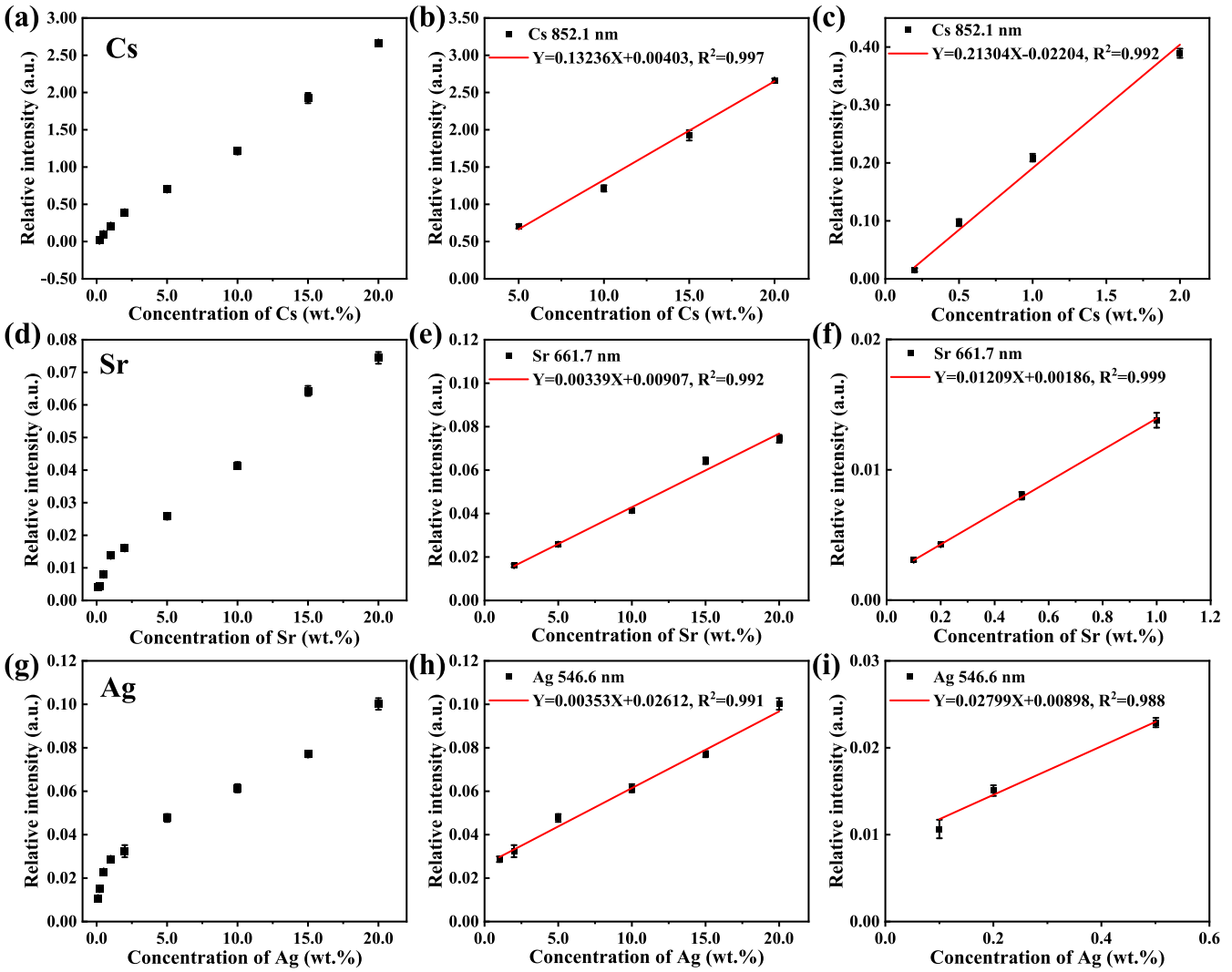

Figure 7. (a), (d), and (g) showed the relationship between the Cs, Sr, and Ag concentrations and the spectral peak relative intensity (Cs 852.1 nm and Ag 546.6 nm used Li 610.4 nm as the internal reference, Sr 661.7 nm used K 766.5 nm as the internal reference), respectively. (b,c), (e,f), and (h,i) illustrated the linear relations of Cs, Sr, and Ag concentrations at different stages, respectively.

%, with linear correlation coefficients (R^2) being 0.997 and 0.992, respectively. Based on the achieved linear regression equation (Figure 7c) at lower Cs concentrations, the LOD for Cs was calculated (LOD = $3\sigma/k$, where k is the slope of the calibration curve in the lower concentration range, and σ is the standard deviation of blank sample measurements conducted continuously 10 times) to be 0.021 wt %. Figure 7e,f was the calibration curves in Sr concentration ranges of 2.0 wt % to 20.0 and 0.1 wt % to 1.0 wt %, with R^2 being 0.992 and 0.999, respectively. Based on the linear regression equation (Figure 7f) at low concentrations, the LOD for Sr was calculated to be 0.073 wt %. Figure 7h,i was the calibration curves in Ag concentration ranges of 1.0 wt % to 20.0 and 0.1 wt % to 0.5 wt %, with R^2 being 0.991 and 0.988, respectively. The LOD for Ag was calculated to be 0.063 wt %.

The quantitative analysis ability of the MIPECA system was fully validated by analysis of the concentration−intensity response relationships of different elements over a large concentration range. The different linear relationship with good R^2 in both high and low concentration ranges indicated that the proposed MIPECA system has good accuracy in element quantitative analysis.

Real-Time Monitoring Performance. Compared with other analytical detection methods, the MIPECA system possesses unique advantages. The microplasma electrode can not only excite atomic emission spectra of elements in molten salt electrolytes but also serve as an electrode to induce reactions and facilitate electrochemical processes. Based on the results of the aforementioned quantitative analysis and considering the distinctive characteristics of microplasma, the MIPECA system holds the potential for real-time monitoring of the types and concentrations of elements during electrochemical reactions. Building on this foundation, we conducted tests to evaluate the real-time monitoring performance of the MIPECA system. Taking into account the electrochemical window of LiCl−KCl molten salt, the standard reduction electrode potentials for various elements, and the antioxidation capabilities of different metals under air conditions, combined with the obtained quantitative analysis data, the electrodeposition process of Ag^+ in LiCl−KCl molten salt was monitored in real-time. Under the function of the microplasma anode, the following reactions will occur in the molten salt:

$$\text{Cathode}: Ag^+ + e^- = Ag\downarrow$$

https://doi.org/10.1021/acs.analchem.4c04004
Anal. Chem. 2024, 96, 20406−20413

$$\text{Anode}: 2Cl^- - 2e^- = Cl_2\uparrow$$

According to Faraday's law:

$$m_f = ItM/zF$$

Where I is the current of electrolysis (mA), t is the electrolytic time (s), F is Faraday's constant, z is the number of electrons transferred in the reaction, and M is the molar mass constant of the metal. During the reaction process, the concentration of Ag^+ in the molten salt linearly decreased over time. Therefore, a concentration of 2.0 wt % Ag^+ was introduced into 2.0 g of LiCl−KCl molten salt, and a constant current of 10 mA was applied for electrolysis. Theoretically, under these conditions, Ag^+ should be depleted in approximately 3600 s. The spectrometer integration time was set to 10 ms with a data acquisition interval of 5 s. Spectral signals were collected throughout the electrolysis process, and the overall electrolysis time was set to 5000 s to ensure a complete reaction of Ag^+.

As shown in Figure 8a, at t = 0 s, a distinct characteristic peak of Ag at 328.1 nm was observed with a significant signal,

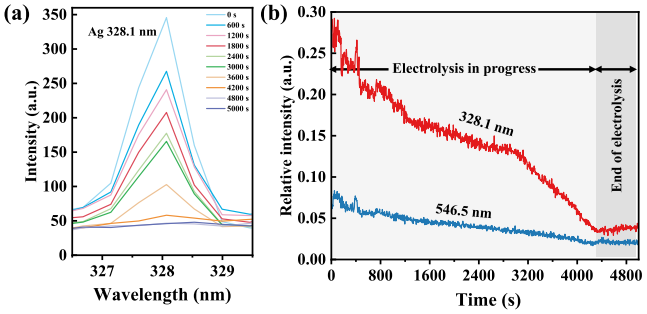

Figure 8. (a) The emission spectrum signal in the range of 326.5−329.5 nm was collected by the MIPECA system at different electrolytic times. (b) The relationship between the relative intensity of Ag characteristic peaks at 328.1 and 546.5 nm and the electrolysis time, with Li 610.4 nm as the internal reference.

far exceeding the background emission. This demonstrated the rapid response capability of the MIPECA system to elemental emission signals. As the electrolysis progressed, the intensity of the characteristic peak at 328.1 nm gradually decreased until it disappeared. Figure 8b detailed the specific variation of the relative intensities of the characteristic peaks at Ag 328.1 and 546.5 nm, using Li 610.4 nm as the internal reference over time. From the result, it was evident that the relative intensity ratio of the two characteristic peaks gradually decreased with ongoing electrolysis and stabilized after 4300 s of electrolysis, indicating the endpoint of the reaction.

Furthermore, the downward trend of the relative intensity over time aligns with the concentration−intensity relationship in the quantitative results. In the electrolysis process, the Ag^+ concentration passes through different stages. According to the quantitative results, the corresponding spectral signal intensity trends were different in different concentration stages. At the beginning of electrolysis, the concentration of Ag^+ was higher, and the signal strength changed slowly with the concentration. With the progress of electrolysis, the concentration of Ag^+ continued to decline and gradually entered the low concentration range, and the changing trend of signal intensity accelerated. Therefore, in this experiment, when electrolysis was carried out around 2800 s, the spectral signal intensity decline rate became faster, suggesting that Ag concentration in molten salt had entered the low concentration range. When the electrolysis reached 4400 s, the spectral signal intensity no longer changed, indicating that the reaction had ended and Ag^+ in the molten salt had been reacted completely. This different intensity trend also indicated that the spectral emission signals during real-time monitoring followed quantitative relationships well. The Ag^+ concentration in the molten salt at each moment could be calculated based on signal intensity, providing robust evidence for the feasibility of the MIPECA system in real-time monitoring of molten salt element concentrations. The experimental results collectively suggest that the MIPECA system has the potential to be a novel online analytical method for molten salt, effectively determining reaction endpoints, observing reaction progress, and analyzing real-time changes in element concentrations within the molten salt.

CONCLUSIONS

Based on the MIPECA system, it is proven that the microplasma cathode can also be used as the excitation source to stimulate the characteristic emission spectrum of molten salt, and the emission spectrum signals of LiCl−KCl molten salt excited by the microplasma electrode under different conditions were also studied. The results indicate that compared to the anode, the cathode exhibits a decrease in the intensity of the characteristic peak of Li. In an argon atmosphere, the microplasma anode distinctly shows the characteristic peak of argon. The effects of discharge distance, molten salt temperature, and current on the strength of the characteristic peaks collected by the MIPECA system were studied, and the operating conditions were optimized. Qualitative analysis of ten elements, including Cs, Na, Mg, Ca, Sr, Ba, Ag, Cu, Ni, and Ce, was successfully conducted. The element characteristic spectral lines of elements with high sensitivity and good stability further expanded the application range of the MIPECA system. The concentration−intensity relationships for Ag, Cs, and Sr in the LiCl−KCl molten salt were determined. The results fully prove the ability of the MIPECA system for quantitative analysis. Building upon this, real-time monitoring of the electrolytic reduction process of Ag^+ was conducted. The relative intensity of Ag's characteristic peak gradually decreased over time, aligning with the quantitative results and showcasing the MIPECA system's capability for real-time monitoring of ion concentration during molten salt electrolysis. Future work will focus on studying the microscopic mechanisms of the MIPECA system and the feasibility of real-time monitoring of actinide and lanthanide elements.

AUTHOR INFORMATION

Corresponding Authors

Zhe Wang − *Institute of Nuclear and New Energy Technology, Tsinghua University, Beijing 100084, China*; Email: wang2023@tsinghua.edu.cn

Yuexiang Lu − *Institute of Nuclear and New Energy Technology, Tsinghua University, Beijing 100084, China*; orcid.org/0000-0003-2755-7733; Email: luyuexiang@mail.tsinghua.edu.cn

Authors

Junhan Luo − *Institute of Nuclear and New Energy Technology, Tsinghua University, Beijing 100084, China*

https://doi.org/10.1021/acs.analchem.4c04004
Anal. Chem. 2024, 96, 20406−20413

Jingcui Liu − *Institute of Nuclear and New Energy Technology, Tsinghua University, Beijing 100084, China*
Qi Qing − *Institute of Nuclear and New Energy Technology, Tsinghua University, Beijing 100084, China*
Shuang Liu − *Nuclear Research Institute for Future Technology and Policy, Seoul National University, Seoul 08826, Republic of Korea*
Jing Chen − *Institute of Nuclear and New Energy Technology, Tsinghua University, Beijing 100084, China*

Complete contact information is available at: https://pubs.acs.org/10.1021/acs.analchem.4c04004

Author Contributions

The manuscript was written through contributions of all authors.

Notes

The authors declare no competing financial interest.

■ ACKNOWLEDGMENTS

This work was financially supported by the National Natural Science Foundation of China (grant nos. 22422606, 22376059), the Young Elite Scientists Sponsorship Program (2021QNRC001) of China Association for Science and Technology, and the Brain Pool program funded by the Ministry of Science and ICT through the National Research Foundation of Korea (grant number: NRF-2022H1D3A2A02051548).

■ REFERENCES

(1) Xi, X.; Feng, M.; Zhang, L.; Nie, Z. *Int. J. Min. Met. Mater.* **2020**, *27* (12), 1599−1617.
(2) Jiao, S.; Jiao, H.; Song, W.; Wang, M.; Tu, J. *Int. J. Min. Met. Mater.* **2020**, *27* (12), 1588−1598.
(3) Sadoway, D. R. *J. Mater. Res.* **1995**, *10* (3), 487−492.
(4) Liu, M.; Steven Tay, N. H.; Bell, S.; Belusko, M.; Jacob, R.; Will, G.; Saman, W.; Bruno, F. *Renewable Sustainable Energy Rev.* **2016**, *53*, 1411−1432.
(5) Masset, P.; Guidotti, R. A. *J. Power Sources* **2007**, *164* (1), 397−414.
(6) Mirza, M.; Abdulaziz, R.; Maskell, W. C.; Wilcock, S.; Jones, A. H.; Woodall, S.; Jackson, A.; Shearing, P. R.; Brett, D. J. L. *Energy Environ. Sci.* **2023**, *16* (3), 952−982.
(7) Yevilevich, Y.; Vradman, L.; Zana, J.; Weinstock, I. A.; Herskowitz, M. *Inorg. Chem.* **2022**, *61* (17), 6367−6375.
(8) Kim, Y. S.; Han, B. Y.; Shin, H. S.; Kim, H. D.; Jung, E. C.; Jung, J. H.; Na, S. H. *Spectrochim. Acta, Part B* **2012**, *74*−*75*, 190−193.
(9) Liu, Y.; Luo, L.; Liu, N.; Yao, B.; Liu, K.; Yuan, L.; Chai, Z.; Shi, W. *J. Nucl. Mater.* **2018**, *508*, 63−73.
(10) Luo, J.; Qing, Q.; Wang, Z.; Liu, S.; Chen, J.; Lu, Y. *Sep. Purif. Technol.* **2024**, *332*, 125829.
(11) Park, J.; Choi, S.; Sohn, S.; Hwang, S., II *J. Electrochem. Soc.* **2017**, *164* (12), D744.
(12) Yoon, S.; Choi, S. *J. Electrochem. Soc.* **2021**, *168*, 013504.
(13) Hull, G.; Lambert, H.; Haroon, K.; Coffey, P.; Kerry, T.; McNaghten, E. D.; Sharrad, C. A.; Martin, P. *J. Anal. At. Spectrom.* **2021**, *36* (1), 92−102.
(14) Lee, Y.; Yoon, S.; Kim, N.; Kang, D.; Kim, H.; Yang, W.; Burger, M.; Jovanovic, I.; Choi, S. *Nucl. Eng. Technol.* **2022**, *54* (12), 4431−4440.
(15) Phongikaroon, S. *Measurement Of Irradiated Pyroprocessing Samples Via Laser Induced Breakdown Spectroscopy*; Virginia Commonwealth University: United States, 2016. https://www.osti.gov/biblio/1333919.
(16) Gruen, D. M. *J. Inorg. Nucl. Chem.* **1957**, *4* (1), 74−76.
(17) Schroll, C. A.; Lines, A. M.; Heineman, W. R.; Bryan, S. A. *Anal. Methods* **2016**, *8* (43), 7731−7738.
(18) Uda, T.; Fujii, T.; Iwadate, Y.; Uehara, A.; Yamana, H. *Z. Anorg. Allg. Chem.* **2013**, *639* (5), 765−769.
(19) Greda, K.; Swiderski, K.; Jamroz, P.; Pohl, P. *Anal. Chem.* **2016**, *88* (17), 8812−8820.
(20) Liu, X.; Liu, Z.; Zhu, Z.; He, D.; Yao, S.; Zheng, H.; Hu, S. *Anal. Chem.* **2017**, *89* (6), 3739−3746.
(21) Peng, X.; Guo, X.; Ge, F.; Wang, Z. *J. Anal. At. Spectrom.* **2019**, *34* (2), 394−400.
(22) Peng, X.; Zhao, M.; Yuan, M.; Wang, Z. *Talanta* **2021**, *225*, 121995.
(23) Davis, W. C.; Marcus, R. K. *J. Anal. At. Spectrom.* **2001**, *16* (9), 931−937.
(24) Greda, K.; Jamroz, P.; Jedryczko, D.; Pohl, P. *Talanta* **2015**, *137*, 11−17.
(25) Peng, X.; Wang, Z. *Anal. Chem.* **2019**, *91* (15), 10073−10080.
(26) Zhu, Z.; Yang, C.; Yu, P.; Zheng, H.; Liu, Z.; Xing, Z.; Hu, S. *J. Anal. At. Spectrom.* **2019**, *34* (2), 331−337.
(27) Cai, Z.; Chen, H.; Gao, M.; Wang, Z. *Talanta* **2024**, *266* (Pt 2), 125111.
(28) Wei, G.; Liu, X.; Lu, Y.; Wang, Z.; Liu, S.; Ye, G.; Chen, J. *Anal. Chem.* **2018**, *90* (22), 13163−13166.
(29) Luo, J.; Qing, Q.; Huang, L.; Wang, Z.; Liu, S.; Chen, J.; Lu, Y. *Chin. Chem. Lett.* **2024**, *35* (4), 108483.
(30) Richards, W. G.; Scott, P. R. *Structure and Spectra of Atoms*; Wiley, 1976.